Separation Science and Technology
Publication details, including instructions for authors and subscription information:
http://www.informaworld.com/smpp/title~content=t713708471

Kinetics of Adsorptive Drying of Isopropyl Alcohol by 4A Molecular Sieve Cylindrical Pellets: Simple Rate Model

Anil K. Jain; Ashok K. Gupta

To cite this Article Jain, Anil K. and Gupta, Ashok K.(1998) 'Kinetics of Adsorptive Drying of Isopropyl Alcohol by 4A Molecular Sieve Cylindrical Pellets: Simple Rate Model', Separation Science and Technology, 33: 5, 683 — 705

To link to this Article: DOI: 10.1080/01496399808544783

URL: http://dx.doi.org/10.1080/01496399808544783

SEPARATION SCIENCE AND TECHNOLOGY, 33(5), pp. 683–705, 1998

Kinetics of Adsorptive Drying of Isopropyl Alcohol by 4A Molecular Sieve Cylindrical Pellets: Simple Rate Model

ANIL K. JAIN and ASHOK K. GUPTA*
DEPARTMENT OF CHEMICAL ENGINEERING
INDIAN INSTITUTE OF TECHNOLOGY, DELHI
HAUZ KHAS, NEW DELHI 110 016, INDIA

ABSTRACT

Batch kinetic studies of the adsorption of water on 4A molecular sieve cylindrical pellets from its solution in isopropyl alcohol, reported earlier, have been mathematically modeled. Each cylindrical pellet was assumed to be composed of microspheres (zeolite crystallites) of equal size. Partial differential equations describing mass transfer in a biporous cylindrical pellet were written and solved numerically to obtain the concentration of adsorbate in the macropores, fractional saturation of individual microspheres, and fractional saturation of the entire pellet. Fractional saturation of microspheres at any instant involves three different regions of the adsorbent pellet: 1) an outer saturated or semisaturated zone, 2) a middle adsorption shell where most of the adsorption is taking place at a given instant. and 3) an unexposed core. The thickness of the adsorption shell decreases as the rate of diffusion (a) increases in the microspheres and (b) decreases in the macropores. This physical picture led to the development of a simpler approximate model which incorporates accumulation in the adsorption shell. This has been named the adsorption shell model. This model is amenable to a hand calculator and could be employed to correlate batch kinetic data.

INTRODUCTION

Biporous solids like zeolite molecular sieves find application in a wide variety of selective adsorption systems. Commercial molecular sieve adsor-

---

* To whom correspondence should be addressed.

bents are generally made from microporous crystals with pore diameters ranging from 3 to 13 Å.

The proper design and optimization of an adsorption separation process requires detailed knowledge of both the equilibrium and kinetic behavior of the system. During the last thirty years many new models and techniques have been proposed. Adsorption kinetics in a biporous cylindrical pellet was considered for the first time by Smith (17). Do (6) analyzed the rate of adsorption of a gas into a bimodal microporous solid with an irreversible isotherm. Riekert (15) suggested the design of experiments such that diffusion in micropores is not affected by mass transfer in macropores. Hyun Kim (8) prescribed a method to calculate single diffusivity parameter for macropores and microspheres of a biporous adsorbent.

Sun et al. (19) used a biporous model which included heat and mass transfer resistances to analyze frequency response for nonisothermal adsorption. Bulow and Micke (3) described a method to determine transport coefficients for molecular sieve systems. Giona et al. (7) proposed a simple macroscopic model to describe adsorption in a molecular sieve pellet. Tantat et al. (20) used a simplified biporous model to calculate mass transfer resistance for SO_2/water vapor adsorption on zeolite. Bourdin et al. (2) proposed a new analytical bidispersed model which delineates heat transfer from mass transfer.

Many researchers have reported studies on adsorptive drying of fluids, e.g., Ruthven and Rojo (16), Naumov et al. (14), Joshi and Fair (11), Sowerby and Crittenden (18), Crittenden and Ben-Shebal (5), Leech (12), and Buragohin et al. (4).

The present work deals with adsorptive drying of isopropyl alcohol by 4A molecular sieve cylindrical pellets. Results of batch kinetic studies we reported earlier (9) have been analyzed by a new and simpler mathematical model. For the sake of continuity, a summary of the work is also being presented here.

Equilibrium data are presented in Fig. 1 At concentrations of water ≥ 0.01 kg/kg IPA in the bulk fluid phase, the amount of water adsorbed is 0.25 kg/kg of molecular sieve. At lower concentrations the amount of water adsorbed varies almost linearly with its concentration in the fluid phase. For simplicity, it was idealized that for any finite concentration of water in the bulk fluid phase, the amount adsorbed per kilogram of adsorbent pellet would be 0.25 kg. This has been termed as rectangular equilibrium behavior.

Batch kinetic experiments were conducted at different initial concentrations of water. The diffusion in a biporous pellet with a cylindrical geometry was considered. To analyze the experimental results, necessary equations were developed and solved numerically. Rectangular boundary condition was assumed while determining the uptake of water by microspheres. Macropore

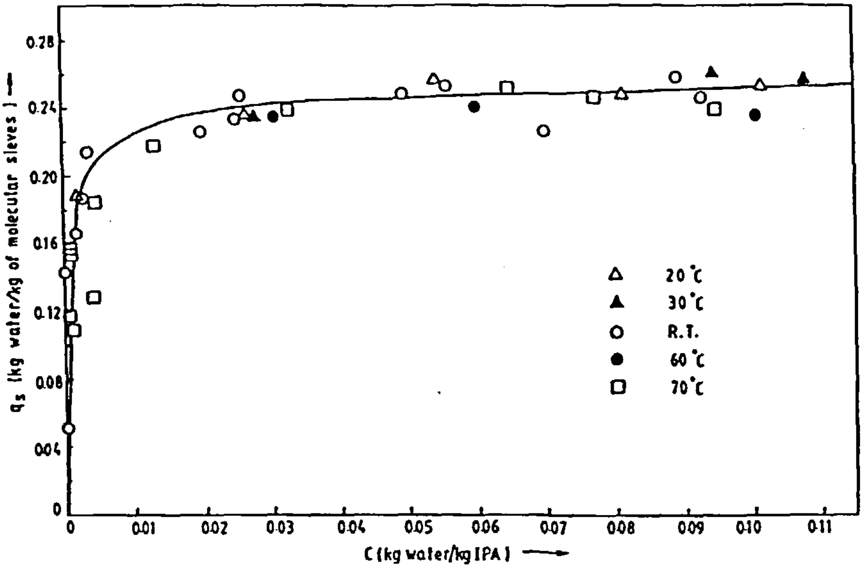

FIG. 1 Experimental equilibrium data for adsorption of water on molecular sieve 4A.

and microsphere diffusion parameters were determined which correlated the experimental data.

All the experimental conditions of the system (viz., macropore and microsphere diffusion parameters, initial concentration of adsorbate in bulk fluid phase, C_0, and adsorption capacity of adsorbent, $(1 - \epsilon)q_0$), could be combined together in terms of a single dimensionless parameter, β, where

$$\beta = \frac{3(1 - \epsilon)q_0 D_c/r_c^2}{\epsilon C_0 D_p/R_p^2}$$

Each term in the above expression is defined in the Nomenclature section. It was observed from the detailed numerical results of mass balance equations (incorporating diffusion in microspheres as well as in macropores) that at a given instant, most adsorption takes place in a narrow region of the pellet. The microspheres constituting a single biporous solid particle could be classified into three distinct regions: 1) the outermost shell of microspheres which is almost equally saturated; 2) the middle adsorption shell of microspheres where most adsorption is taking place, and 3) the inner core of microspheres which is yet to be exposed to the adsorbate. The thickness of the adsorption shell decreases as the value of β increases. This point is elaborated later in the section titled "Simultaneous Diffusion in Macropores and Microspheres."

AIM AND SCOPE

The above analysis requires large computer time, sometimes up to more than 1 CPU hour on an ICL 3980 mainframe computer. This led to the development of a semiempirical model, called the adsorption shell model, which is amenable to hand computations.

A similar model was developed earlier for biporous spherical particles (1). Originally the model was developed for values of $\beta \rightarrow \infty$. For this situation, most adsorption takes place in a thin adsorption shell. It was observed that the model could correlate the experimental data for systems with values of β varying over a wide range: $\beta \simeq 30$, adsorption of water vapor by molecular sieve 4A; $\beta \simeq 1{,}000-10{,}000$, sorption of NaOH by a strongly acidic macroreticular ion-exchange resin; $\beta = 10{,}000-15{,}000$, sorption of H_2SO_4 by a strongly basic macroreticular ion-exchange resin; $\beta \simeq 130{,}000$, sorption of dissolved oxygen by the sulfite form of a strongly basic macroreticular ion-exchange resin. It should be emphasized this model will be valid when the adsorption equilibrium is of the rectangular type.

It was decided to develop a similar model for cylindrical geometry and to explore the feasibility of correlating the experimental kinetic data of the present system, i.e., adsorptive drying of isopropyl alcohol on molecular sieve 4A. Adsorption of water on molecular sieve 4A is almost rectangular.

BACKGROUND

When a biporous solid particle is exposed to the adsorbate, it tends to diffuse inward through the macropores. The concentration of adsorbate in the macropores, θ_p, decreases as one moves toward the center from the outside. Also, the average fractional saturation of individual microspheres, $\overline{\theta}_c$, will increase with time. A schematic diagram of a biporous pellet representing macropores and microspheres is given in Fig. 2.

The mass balance equations are

$$\frac{\epsilon D_p}{R}\frac{\partial}{\partial R}\left[R\frac{\partial C}{\partial R}\right] = \epsilon\frac{\partial C}{\partial t} + (1-\epsilon)\frac{\partial \overline{q}}{\partial t} \tag{1}$$

$$\frac{\partial q}{\partial t} = \frac{D_c}{r^2}\frac{\partial}{\partial r}\left(r^2\frac{\partial q}{\partial r}\right) \tag{2}$$

$$\overline{q} = \frac{3}{r_c^3}\int_0^{r_c} qr^2\,dr \tag{3}$$

The two terms on the RHS of Eq. (1) represent accumulation in macropores and microspheres, respectively. Equation (2) corresponds to the mass balance

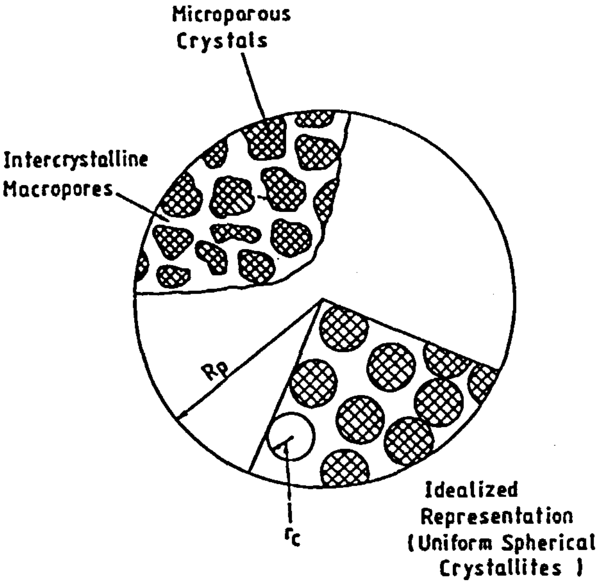

FIG. 2 Schematic diagram of composite adsorbent pellet.

in a microsphere; Eq. (3) represents average concentration of adsorbate in a microsphere.

$$\text{I.C.} \qquad t \leq 0,\ C(R, 0) = 0, \qquad q(r, 0) = 0 \text{ for all } R$$

$$\text{B.C.} \qquad t > 0,\ C(R_p, t) = C_0[1 - \Lambda U(t)], \qquad \left.\frac{\partial C}{\partial R}\right|_{R=0} = 0 \text{ for all } t$$

$$q(r_c, t) = q_0 \text{ when } C(R, t) > 0, \qquad \left.\frac{\partial q}{\partial r}\right|_{r=0} = 0 \text{ for all } t$$

where

$$\Lambda = \frac{mq_s}{V_L C_0} = \frac{\text{total adsorption capacity of adsorbent}}{\text{amount of adsorbate initially present in solution}}$$

Mass balance equations in dimensionless form for diffusion in cylindrical biporous pellets are

$$\frac{1}{\eta}\frac{\partial}{\partial \eta}\left[\eta \frac{\partial \theta_p}{\partial \eta}\right] = \alpha \frac{\partial \theta_p}{\partial \tau} + \frac{\beta}{3}\frac{\partial \bar{\theta}_c}{\partial \tau} \tag{4}$$

$$\text{I.C.} \qquad \theta_p(\eta, 0) = 0, \qquad \theta_c(\gamma, 0) = 0 \text{ for all } \eta$$

$$\text{B.C.} \quad \theta_p(1, \tau) = 1 - \Lambda U(\tau), \qquad \left.\frac{\partial \theta_p}{\partial \eta}\right|_{\eta=0} = 0$$

The first term on the RHS of Eq. (4) represents accumulation in the macropores, and the second term, accumulation in microspheres.

Equations describing diffusion in a microsphere can also be written in dimensionless form:

$$\frac{\partial}{\partial \gamma}\left[\gamma^2 \frac{\partial \theta_c}{\partial \gamma}\right] = \frac{\partial \theta_c}{\partial \tau} \tag{5}$$

$$\bar{\theta}_c = 3 \int_0^1 \theta_c \gamma^2 \, d\gamma$$

$$\text{I.C.} \quad \theta_c(\gamma, 0) = 0 \text{ for all } \eta$$

$$\text{B.C.} \quad \theta_c(1, \tau) = 1 \text{ for } \theta_p > 0 \text{ for all } \eta$$

(rectangular boundary condition;

the present experimental system shows this behavior)

$$\left.\frac{\partial \theta_c}{\partial \gamma}\right|_{\gamma=0} = 0 \text{ for all } \eta$$

Equations (4) and (5) along with appropriate initial and boundary conditions completely describe the adsorption in a cylindrical pellet. These were solved numerically by the explicit forward difference method. A computer program was developed to generate concentration profile in macropores, fractional saturation of individual microspheres, and fractional saturation of the entire pellet. In the numerical computations the radius of the cylindrical pellet was divided into 50 parts. Computation time on an ICL 3980 mainframe computer exceeded 1 CPU hour to compute 90% fractional saturation.

SIMULTANEOUS DIFFUSION IN MACROPORES AND MICROSPHERES

The parameter β is a combination of all the parameters influencing the rate of adsorption. Increases in the values C_0, D_p/R_p^2, and D_c/r_c^2 would increase the rate of adsorption. A large value of β implies that the characteristic time of a microsphere, r_c^2/D_c is very small compared to the characteristic time of the pellet, $R_p^2(1 - \epsilon)q_0/D_p\epsilon C_0$. In the present analysis the computations were performed for the values of β varying over a large range (~0 to more than 100).

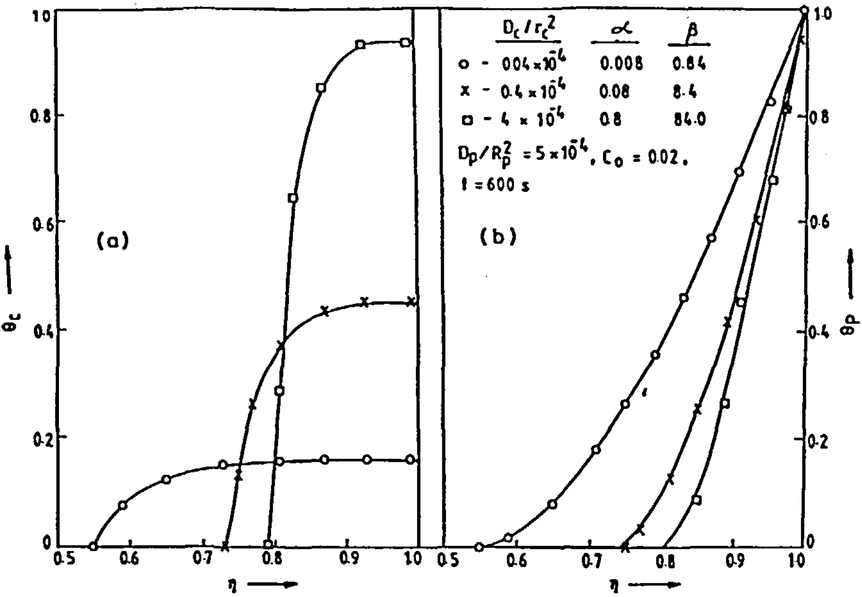

FIG. 3 Adsorption in a biporous cylindrical pellet: Computed results. (a) Fractional saturation of microspheres. (b) Concentration profile in macropores.

Some representative results are shown in Fig. 3 The concentration profile in macropores and the fractional saturation of individual microspheres at different radial positions are shown. For a given value of β, $\bar{\theta}_c$ is almost the same up to a certain depth in the pellet, and then it sharply decreases to zero. Also, at any particle surface, i.e., $\eta = 1$, $\bar{\theta}_c$ increases with an increase in β. However, the extent to which the adsorbate has penetrated the pellet decreases with an increase in β. Also, it will take some time before the adsorbate reaches the center of the pellet and all microspheres are exposed to the adsorbate. Thus, microspheres may belong to any one of three regions.

1. *Outer shell of saturated or semisaturated microspheres*: Fractional saturation of individual microspheres, $\bar{\theta}_c$, is almost equal. Thickness of this shell increases with time.
2. *Middle adsorption shell of partially saturated microspheres*: Microspheres where most adsorption is taking place at a given instant. $\bar{\theta}_c$ values for individual microspheres toward the outer side are slightly less than that in the outer shell and decrease to zero inward. Thickness of adsorption shell would depend on the value of β; the larger the value of β, the

thinner the adsorption shell. This adsorption shell "moves" toward the center with time.

3. *Unexposed inner core*: Microspheres which are yet to be exposed to the adsorbate. The radius of this core will decrease with time.

These observations are shown schematically in Fig. 4. The existence of the three regions is similar to adsorption in a packed bed: saturated zone, adsorption zone, and zone free of adsorbate (22). As mentioned earlier, computations by rigorous analysis, i.e., numerical solution of partial differential equations, requires enormous efforts in terms of computation time Also, most adsorption is taking place at a given instant in the adsorption shell. By incorporating this particular phenomenon, an approximate analysis has been developed. The focal point is to determine the concentration gradient of the adsor-

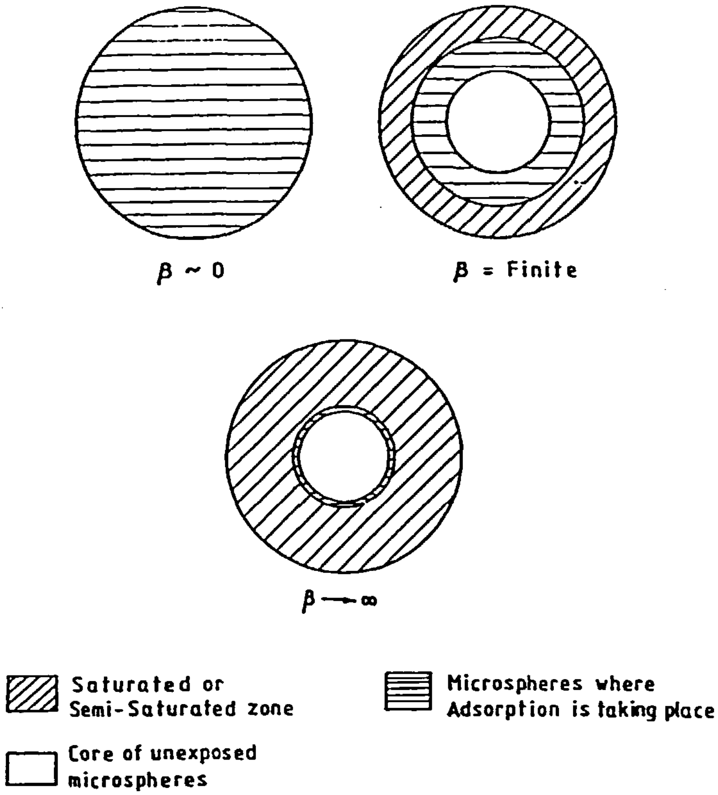

FIG. 4 Adsorption shell (schematic): Effect of β.

bate in the macropores *at the interface between outer shell and adsorption shell,* and hence to express accumulation in the adsorption shell in terms of parameter β. For mathematical simplicity, it has been idealized that $\beta \rightarrow \infty$, i.e., diffusion in microspheres is very rapid as compared to that in macropores. This implies that the outer shell is completely saturated ($\bar{\theta}_c \simeq 1$) and that the adsorption shell is very thin.

MATHEMATICAL DEVELOPMENT

Approximate Analysis for $\beta \rightarrow \infty$: Adsorption Shell Model

The analysis has been developed both for (a) unchanging bulk fluid phase composition, i.e., infinite solution volume condition, and for (b) changing concentration of adsorbate in the bulk fluid phase due to finite solution volume.

Infinite Solution Volume Condition

It is assumed that the concentration profile of adsorbate in the macropores at any time is as shown in Fig. 5. The following picture over a short interval of time is hypothesized.

1. An outer shell of saturated microspheres ($\bar{\theta}_c = 1$) extending from dimensionless radius $\eta = 1$ to dimensionless radius $\eta = \eta_c^+$ exists. The concentration of the adsorbate in the macropores changes very gradually (quasi-steady state). The thickness of this shell, $1 - \eta_c^+$, increases with time.
2. A thin shell of microspheres of thickness $(\eta_c^+ - \eta_c)$, where most of the adsorption at a given instant is actually taking place, exists, and over short intervals of time the concentration of adsorbate in the macropores does not change (quasi-steady-state situation). The average fractional saturation of the microsphere, $\bar{\theta}_c$, increases with time, $0 \leq \bar{\theta}_c \leq 1$. This shell "moves" toward the center with time.
3. A core of microspheres of dimensionless radius η_c yet to be exposed to the solute exists, i.e., $\theta_p = 0$, $\theta_c = 0$.

For a very thin adsorption shell, i.e., $(\eta_c^+ - \eta_c) \ll 1$

$$\begin{array}{l}\text{Fractional saturation} \\ \text{of the pellet, } U\end{array} = \frac{\text{volume of saturated microspheres}}{\text{cumulative volume of all microspheres}}$$

$$= 1 - \eta_c^2$$

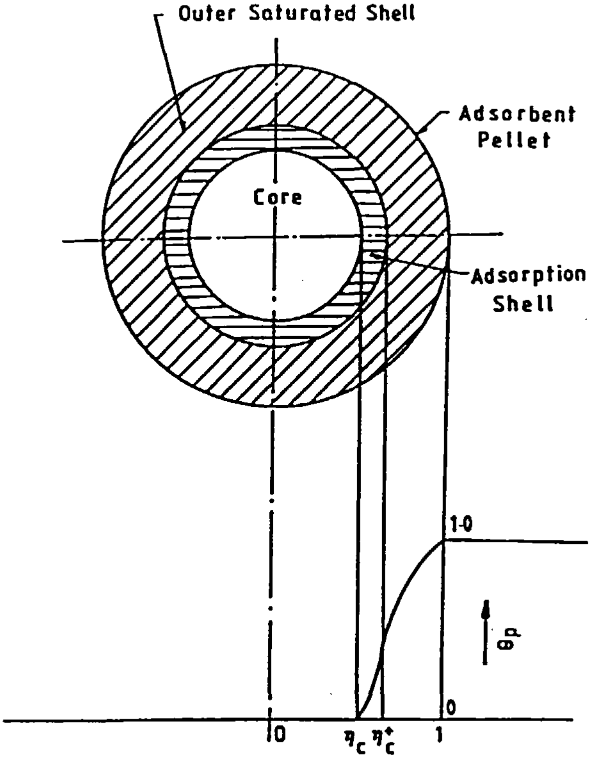

FIG. 5 Concentration profile of adsorbate in the macropores for a large value of β: Adsorption shell model.

Fractional saturation of the pellet will increase with time. The contribution of microspheres in the adsorption shell would be very small toward fractional saturation of the pellet.

Thus the following may be stated.

Outer Saturated Shell: $1 > \eta > \eta_c^+$, $\bar{\theta}_c = 1$

$$d\theta_p/d\tau = 0,\ d\bar{\theta}_c/d\tau = 0 \text{ (quasi-steady state)}$$

For the given situation, Eq. (4) reduces to

$$\frac{1}{\eta}\frac{d}{d\eta}\left[\eta\,\frac{d\theta_p}{d\eta}\right] = 0 \qquad (6)$$

or

$$\eta \frac{d\theta_p}{d\eta} = \text{constant} \tag{7}$$

$$\text{B.C.} \quad \eta = 1,\ \theta_p = 1$$

$$\eta = \eta_c^+,\ \theta_p = 0^+$$

Adsorption Shell: $\eta_c^+ > \eta > \eta_c$, $1 \geq \bar{\theta}_c \geq 0$

It is intended to determine the concentration gradient of adsorbate in the macropores in the adsorption shell.

$$d\theta_p/d\tau = 0 \text{ (quasi-steady state)}$$

Adsorbate reaching a given location per unit time is proportional to the surface area of a cylindrical shell which is proportional to η. We assume that accumulation in the microspheres of the adsorption shell is proportional to the radial position, i.e.,

$$\frac{\beta}{3}\frac{d\bar{\theta}_c}{d\tau} = K\eta \tag{8}$$

where K is a constant of proportionality termed "accumulation parameter."

Therefore, Eq. (4) may be rewritten as

$$\frac{1}{\eta}\frac{d}{d\eta}\left[\eta \frac{d\theta_p}{d\eta}\right] = K\eta \tag{9}$$

or

$$\frac{d}{d\eta}\left[\eta\frac{d\theta_p}{d\eta}\right] = K\eta^2 \tag{10}$$

$$\text{B.C.} \quad \eta = \eta_c,\ \theta_p = 0$$

$$\eta = \eta_c^+,\ \theta_p = 0^+$$

Integrating Eq. (10) and simplifying, we get

$$\frac{d\theta_p}{d\eta} = \frac{K\eta^2}{3} + \frac{K_1}{\eta}$$

$$d\theta_p/d\eta = 0 \text{ at } \eta = 0 \text{ (radial symmetry)}, \therefore K_1 = 0$$

Therefore

$$d\theta_p/d\eta = K\eta^2/3 \tag{11}$$

or

$$\left.\frac{d\theta_p}{d\eta}\right|_{\eta_c^+} = \frac{K}{3}\eta_c^{+2} \tag{12}$$

Equation (12) gives the concentration gradient of adsorbate at the boundary of the adsorption shell.

Figure 5 shows the concentration profile as indicated by Eqs. (6), (7), (11), and (12).

The Adsorption Shell Moves as a Front, Its Dimensionless Thickness Being $\eta_c^+ - \eta_c$

Also, moles of adsorbate reaching the surface of an adsorption cylindrical shell per unit time = moles of adsorbate required to decrease the volume of the unexposed core. This approach is the same as that reported in the literature (13, 21). That is,

$$2\pi LR\epsilon D_p \left.\frac{dC}{dR}\right|_{R_c^+} = \frac{-d}{dt}(\pi R_c^2 L(1-\epsilon)q_0)$$

$$= -2\pi R_c L(1-\epsilon)q_0 \frac{dR_c}{dt}$$

Therefore

$$D_p \left.\frac{dC}{dR}\right|_{R_c^+} = -\frac{(1-\epsilon)q_0}{\epsilon}\frac{dR_c}{dt} \qquad (R_c^+ \simeq R_c) \tag{13}$$

or

$$\left.\frac{d\theta_p}{d\eta}\right|_{\eta_c^+} = -\frac{(1-\epsilon)q_0 R_p}{\epsilon C_0 D_p}\frac{dR_c}{dt} \tag{14}$$

The RHS of Eq. (14) may be rewritten as

$$-\frac{(1-\epsilon)q_0 R_p}{\epsilon C_0 D_p} R_p \frac{d(R_c/R_p)}{dt} = -\frac{\beta}{3}\frac{d\eta_c}{d\tau}$$

Therefore

$$\left.\frac{d\theta_p}{d\eta}\right|_{\eta_c^+} = -\frac{\beta}{3}\frac{d\eta_c}{d\tau} \tag{15}$$

Equation (15) gives the concentration gradient of adsorbate at the interface between the adsorption shell and the saturated shell.

Note that the concentration gradient of the adsorbate at η_c^+, the interface between the outer saturated shell and the adsorption shell, will be the same whether it is approached from the "saturated shell" side or from the "adsorption shell" side. The former is given by Eq. (15) and the latter by Eq. (12).

Equating Eqs. (12) and (15) and eliminating $(d\theta_p/d\eta)|_{\eta_c^+}$:

$$-\frac{\beta}{3}\frac{d\eta_c}{d\tau} = \frac{K\eta_c^{+2}}{3} \tag{16}$$

$$\eta_c^+ \simeq \eta_c \text{ (thin adsorption shell)}$$

That is,

$$-\frac{\beta}{3}\frac{d\eta_c}{d\tau} = \frac{K\eta_c^2}{3} \tag{17}$$

or

$$\frac{d\eta_c}{\eta_c^2} = -\frac{K}{\beta}\,d\tau$$

Integrating:

$$-\frac{1}{\eta_c}\Big|_1^{\eta_c} = -\frac{K}{\beta}\tau \quad \text{or} \quad \left[\frac{1}{\eta_c} - 1\right] = \frac{K}{\beta}\tau \tag{18}$$

Since

$$U = 1 - \eta_c^2, \therefore \eta_c = \sqrt{1 - U} \tag{19}$$

where η_c is the dimensionless radius of the unexposed core.

Equation (18) may be rewritten as

$$\frac{1}{\sqrt{1 - U}} - 1 = \frac{K}{\beta}\tau \tag{20}$$

Rearranging Eq. (20) and simplifying, we get

$$U = 1 - \left[\frac{1}{1 + [(K/\beta)(D_c/r_c^2t)]}\right]^2 \tag{21}$$

To examine the validity of Eq. (21), U vs t results available from rigorous

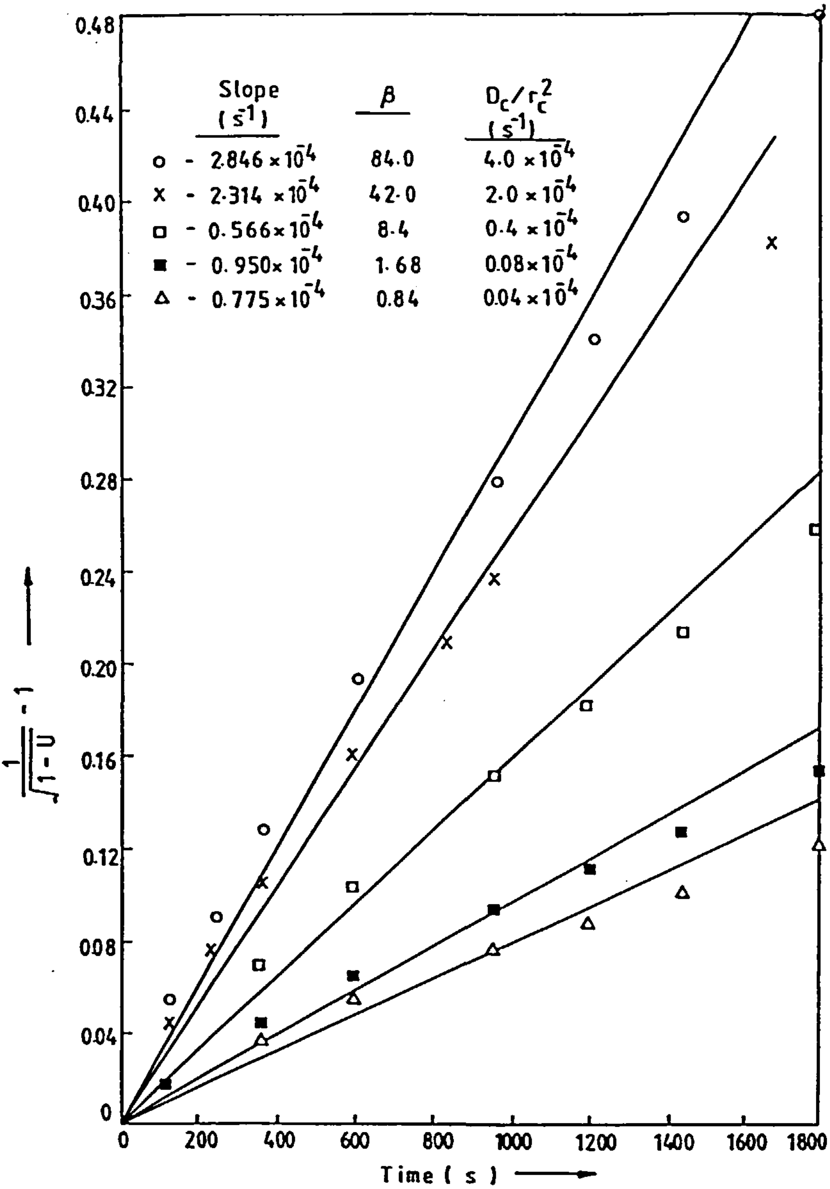

FIG. 6 Rate of adsorption at various values of β: Adsorption shell model.

TABLE 1
Approximate Analysis: β and Corresponding Dimensionless Accumulation Parameter K

β	D_c/r_c^2 (s^{-1})	K/β, D_c/r_c^2 (s^{-1})	K/β	K
0.840	0.04×10^{-4}	0.775×10^{-4}	19.275	16.27
1.680	0.08×10^{-4}	0.953×10^{-4}	11.875	19.95
8.400	0.4×10^{-4}	1.562×10^{-4}	2.915	32.88
16.800	0.8×10^{-4}	2.064×10^{-4}	2.580	43.34
42.000	2.0×10^{-4}	2.315×10^{-4}	1.155	48.51
84.000	4.0×10^{-4}	2.841×10^{-4}	0.711	57.76

computation were used to calculate $[(1/\sqrt{1-U})-1]$ and plotted against t for different values of β, and straight lines were drawn (Fig. 6). The numerical results do not fall very strictly on the straight lines. As expected, there is some deviation because the proposed approximate analysis would be exactly valid only for very large values of β. Note also that a large value of β means a thin adsorption shell and a saturated outer shell.

The slopes of the plots, i.e., K/β, D_c/r_c^2, and values of K for different values of β (0.84 to 84), are shown in Table 1. At lower values of β, K/β decreases markedly with an increase in β. However, at higher values of β, the variation is not significant. In general, the parameter K increases with an increase in β. Thus, knowing the value of K, the concentration gradient of adsorbate in macropores at the outer boundary of an adsorption shell can be determined (Eq. 12). Also, lower values of β (or K) mean a wider adsorption shell. This implies that at lower values of β the rate of adsorption depends upon K/β, D_c/r_c^2, or diffusion in both macropores and microspheres. However, at higher values of β, i.e., a narrow adsorption shell, it is mainly governed by D_c/r_c^2 or diffusion phenomenon in the microsphere since K/β does not alter significantly.

Relation between Accumulation Parameter, K, and β

To make use of the present analysis, i.e., to predict fractional saturation of adsorbent pellets, the value of K for the given experimental conditions should be known. Values of K corresponding to different values of β are presented in Table 1.

An empirical relation between K and β may be expressed as

$$K = \frac{14.493\beta}{1 + 0.290\beta} \tag{22}$$

This suggests that for large values of β

1. $K \rightarrow 50$
2. Concentration gradient of adsorbate in macropores at the outer boundary of an adsorption shell for a given fractional saturation is independent of β

It may therefore be summarized that knowing the values of the individual parameters, viz., ϵ, C_0, $(1 - \epsilon)q_0$, D_p, R_p, D_c/r_c^2, fractional saturation at different times can be computed with the help of Eqs. (21) and (22).

Finite Solution Volume Condition

The foregoing analysis should be applicable for the infinite solution volume condition. However, experimental kinetic data with liquids are available for the finite solution volume condition only. The concentration of adsorbate, C_t, in solution at any time is given by

$$V_L(C_0 - C_t) = V_m(1 - \epsilon)q_0 U$$

$$U = 1 - \eta_c^2$$

or

$$V_L(C_0 - C_t) = V_m(1 - \epsilon)q_0(1 - \eta_c^2) \tag{23}$$

That is,

$$\theta_p = 1 - \Lambda U(\tau) \text{ at } \eta = 1 \tag{24}$$

Incorporating this condition, it can be shown that fractional saturation of a pellet would be predicted for a given set of experimental conditions by the following expression:

$$\left[\frac{1}{\eta_c} - 1\right] + \frac{1}{b}\left[\tan^{-1}\frac{\eta_c}{b} - \tan^{-1}\frac{1}{b}\right] = (1 - \Lambda)\frac{K}{\beta}\tau = \frac{(1 - \Lambda)\epsilon C_0 D_p K}{3(1 - \epsilon)q_0 R_p^2}t \tag{25}$$

where $b = \sqrt{(1 - \Lambda)/\Lambda}$.

This expression is valid for $\Lambda < 1$. It is obvious that the smaller the value of Λ, the closer it will approach Eq. (18), i.e., infinite solution volume condition.

Verification from Experimental Data

Batch kinetics data (9, 10) for drying isopropyl alcohol on a 4A molecular sieve have been considered for verification of the foregoing analysis. Values of the different parameters are listed in Table 2.

For any experimental run, U and t are known and the function on the LHS of Eq. (25) can be generated. For example, for Run 5, $C_0 = 0.0602 \times 10^3$ kg/m^3, $\Lambda = 0.318$, $b = 1.4645$, $(1 - \epsilon)q_0 = 0.29 \times 10^3$ kg/m^3, $\epsilon = 0.236$, $D_p/R_p^2 = 5.73 \times 10^{-4}$ s^{-1}, and $D_p = D_m/\chi$. The function F varies linearly with time, indicating the validity of Eq. (25) (Fig. 7). The slope of the plot

TABLE 2
Experimental Conditions for Batch Kinetics of Water–Isopropyl Alcohol Mixture and 4A Molecular Sieve System (9, 10)

Run	Initial concentration ($\times 10^{-3}$ kg/m^3)	Final concentration ($\times 10^{-3}$ kg/m^3)	Amount of IPA solution ($\times 10^3$ kg)	Amount of adsorbent ($\times 10^3$ kg)	Λ
2	0.0477	0.0306	149.585	13.731	0.3930
5	0.0602	0.0431	149.646	13.683	0.3180
6	0.0527	0.0398	152.463	9.937	0.2544
8	0.0508	0.0376	150.067	10.002	0.2687
9	0.0509	0.0311	150.204	14.986	0.4032
10	0.0516	2.36×10^{-3}	101.877	31.377	0.9587

is 2.176×10^{-4} s^{-1}. By substituting for $(1 - \Lambda)$, ϵ, $(1 - \epsilon)q_0$, D_p/R_p^2, and C_0, the value of K obtained was 34.8 and the corresponding value of β is 7.90 (Eq. 22). The value of D_c/r_c^2 was found to be 0.724×10^{-4} s^{-1} from the expression of β. Table 3 shows the values of $(K/\beta)(1 - \Lambda)D_c/r_c^2$ determined from the slope, and the values of K, β, and D_c/r_c^2 for different experimental runs determined with the help of the above approach. It is interesting to note that the values of D_c/r_c^2 lie in a narrow range, except for Run 6. The value $D_c/r_c^2 = 0.8 \times 10^{-4}$ s^{-1} was used earlier in rigorous analysis to correlate the computed results with experimental data (10). The values of β for $D_c/r_c^2 = 0.8 \times 10^{-4}$ s^{-1} are also given in Table 3 for comparison. This suggests that Eq. (25) gives results similar to the rigorous numerical method.

Note that the concentration of adsorbate in the bulk fluid decreases with time. Hence the effective value of β increases. Also, because of this, the concentration gradient at the surface tends to "flatten" [i.e., $(\partial\theta_p/\partial\eta)|_{\eta=1} \rightarrow 0$]. This results in a decrease in flux inward. It suggests that accumulation in a thin shell at the particle surface approachs zero. Mathematically, this condition makes Eq. (6) valid. Thus, a finite solution volume condition "creates" a condition equivalent to $\beta \rightarrow \infty$.

Limitation of the Approach

It has been shown earlier that the value of K can be obtained for a given value of β with the help of Eq. (22). However, it may be unreliable to obtain the value of β from the value of K arrived at from the results of a particular erroneous batch kinetic run. A small error in the value of K would be magnified in the value of β. For instance, in the present studies, it would be inappropriate to arrive at the value of β (or D_c/r_c^2) from the results of Run 6.

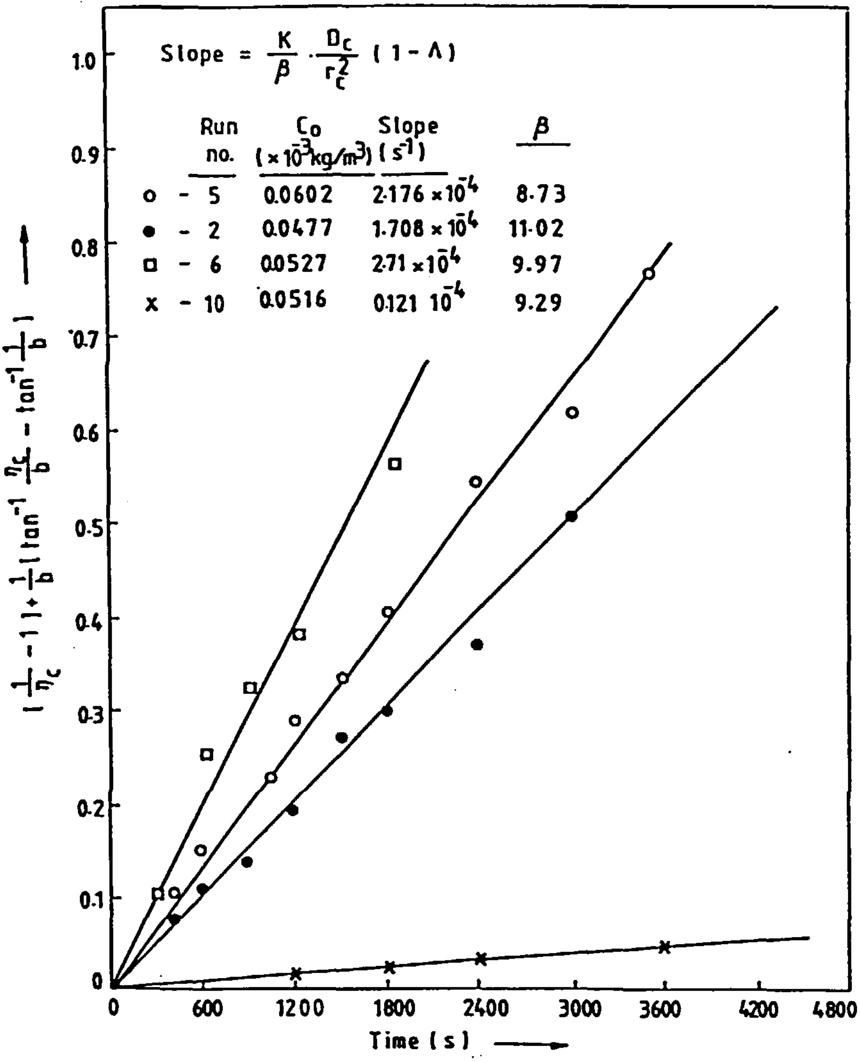

FIG. 7 Approximate analysis of batch kinetic experiments: Adsorption of water on 4A molecular sieve.

TABLE 3

Adsorption Shell Model: Approximate Analysis for Batch Kinetics Experiments

Run	C_0 (m^3/m^3)	Λ	$(K/\beta)(1-\Lambda)D_c/r_c^2$	K (expt)	β^a	D_c/r_c^2 (s^{-1})	β (rigorous analysis)
2	0.0477	0.3930	1.708×10^{-4}	38.78	11.92	0.865×10^{-4}	11.02
5	0.0602	0.3180	2.176×10^{-4}	34.80	7.89	0.723×10^{-4}	8.73
6	0.0527	0.2544	2.71×10^{-4}	45.00	31.05	2.330×10^{-4}	9.97
8	0.0508	0.2687	2.25×10^{-4}	39.76	13.40	1.041×10^{-4}	10.34
9	0.0509	0.4032	1.61×10^{-4}	34.80	7.89	0.611×10^{-4}	10.32
10	0.0516	0.9587	0.121×10^{-4}	34.20	7.47	0.642×10^{-4}	9.29

[a] Approximate analysis values.

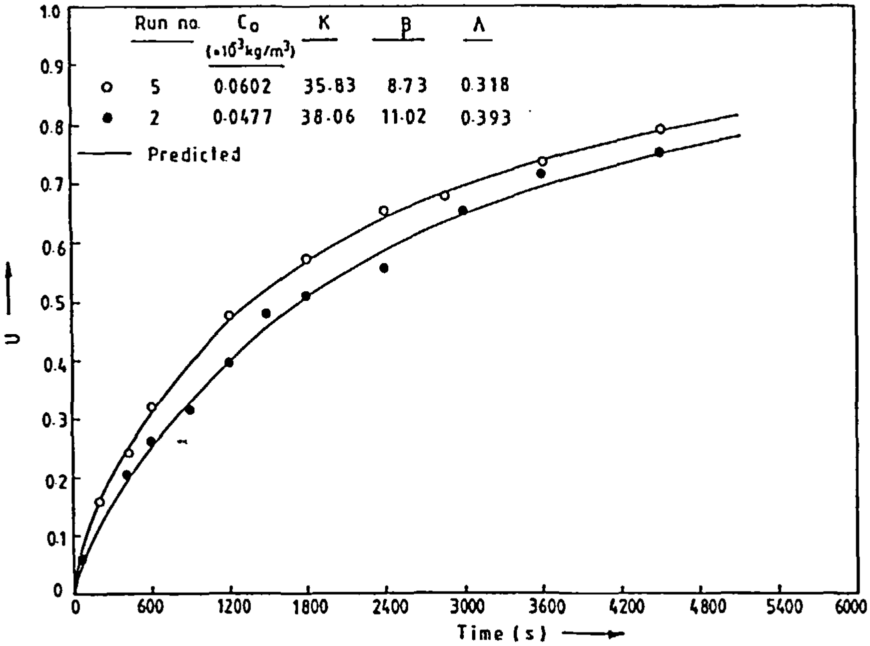

FIG. 8 Analysis of batch kinetic experiments: Prediction by adsorption shell model.

Prediction of Fractional Saturation for Batch Kinetic Experiments

In Eq. (25) all parameters are known except η_c and t. Values of U as 0.05, 0.1, 0.2, 0.3, . . . , 0.9 were assumed and the respective values of $\eta_c = \sqrt{1 - U}$ were calculated. Using appropriate values of Λ, ϵ, C_0, $D_p/R_p^2 = 5.73 \times 10^{-4}\ \mathrm{s}^{-1}$, $(1 - \epsilon)q_0$, and $D_c/r_c^2 = 0.8 \times 10^{-4}\ \mathrm{s}^{-1}$, values of β and K were calculated. The corresponding values of the LHS of Eq. (25) and t were calculated. Fractional saturation values determined with this approach match very well with experimental data (Figs. 8 and 9). Thus it may be concluded that fractional saturation values can be obtained by hand computations.

Although this analysis was developed with the assumption that the adsorption shell is very thin (or $\beta \rightarrow \infty$), in the present case the value of $\beta \cong 10$. This indicates that this model is not very sensitive to β. Thus this model can be very gainfully employed over a wide range of values of β.

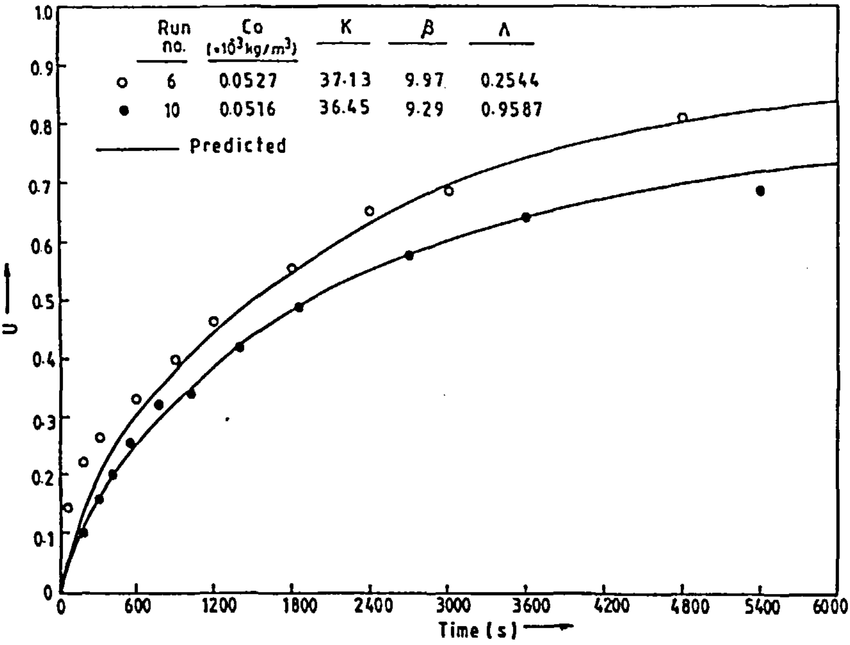

FIG. 9 Analysis of batch kinetic experiments: Prediction by adsorption shell model.

SUMMARY

An adsorption shell model has been developed for adsorption on a biporous cylindrical pellet for the infinite solution volume condition and for the finite solution volume condition. This model is an approximation of rigorous analysis for the same geometry. Knowing the characteristics of the experimental system, viz., ϵ, C_0, Λ, D_p/R_p^2, $(1 - \epsilon)q_0$, and D_c/r_c^2, the value of parameter β can be evaluated, and hence the value of the accumulation parameter K can also be calculated with the help of Eq. (22). Thus, by employing Eq. (25), the fractional saturation of an adsorbent can be predicted by using a hand calculator.

NOMENCLATURE

b	constant $[(1 - \Lambda)/\Lambda]^{1/2}$
C	fluid phase concentration of adsorbate at any radial position R in macropores (kg/m^3 of liquid mixture)
C_0	initial concentration of adsorbate in bulk fluid phase (kg/m^3 mixture)
C_t	concentration of adsorbate in bulk fluid phase at time t
D_c	microsphere diffusivity (m^2·s^{-1})
D_m	molecular diffusivity of the adsorbate in bulk fluid phase (m^2·s^{-1})
D_p	macropore diffusivity (m^2·s^{-1})
F	function, LHS of Eq. (25)
K	accumulation parameter (Eq. 8)
L	length of pellet (m)
m	mass of adsorbent (kg)
q	concentration of adsorbate at any position in a microsphere (Eq. 2)
$\overline{q}$	concentration of adsorbate averaged over a microsphere (Eq. 3)
q_0	adsorbent capacity (kg/m^3 of microsphere volume)
q_s	adsorption capacity (kg/kg of adsorbent)
r	radial coordinate (microsphere)
r_c	microsphere radius (m)
R	radial coordinate (macropore)
R_c	radius of unexposed core
R_c^+	outer radius of adsorption shell (m)
R_p	radius of cylindrical pellet (m)
t	time (s)
U	fractional saturation of adsorbent
V_L	amount of liquid mixture (m^3)
V_m	volume of adsorbent (m^3)

Greek Symbols

α	$D_cR_p^2/D_pr_c^2$, ratio of diffusional time constants
β	$3(1-\epsilon)q_0\alpha/\epsilon C_0$, dimensionless diffusion parameter
γ	r/r_c, dimensionless radial coordinate in microsphere
η	R/R_p, dimensionless radial coordinate in macropore
η_c	$[1-U(t)]^{1/2}$, dimensionless radius of unexposed core
η_c^+	dimensionless outer radius of adsorption shell (Fig. 5)
τ	tD_c/r_c^2, dimensionless time
θ_p	C/C_0, dimensionless concentration in macropore
θ_c	q/q_0
$\bar{\theta}_c$	$\bar{q}/q_0$, fractional saturation averaged over a microsphere, at any η
ϵ	voidage of pellet or macroporosity
Λ	mq_s/V_LC_0, ratio of adsorption capacity of the adsorbent to total adsorbate initially present in solution
χ	tortuosity factor

Other Symbols

B.C.	boundary condition
I.C.	initial condition
IPA	isopropyl alcohol
LHS	left-hand side
RHS	right-hand side

ACKNOWLEDGMENTS

The authors acknowledge the valuable suggestions made by Professor K. Vasudeva, Department of Chemical Engineering, Indian Institute of Technology, New Delhi. A.K.J. acknowledges financial help given in the form of a Research Associateship by the Council of Scientific and Industrial Research (CSIR), India.

REFERENCES

1. N. Anand, B. G. R. Manoja, and A. K. Gupta, *Chem. Eng. Sci.*, *49*(19), 3277 (1994).
2. V. Bourdin, Ph. Grenier, F. Meunier, and L. M. Sun, *AIChE J.*, *42*(3), 700 (1996).
3. M. Bulow and A. Micke, *Adsorption*, *1*(1), 29 (1995).
4. P. V. Buragohin, W. N. Gill, and S. M. Cramer, *Ind. Eng. Chem. Res.*, *35*(9), 3149 (1996).
5. B. D. Crittenden and S. Ben-Shebal, *Inst. Chem. Eng. Symp. Ser.* 2(129), 1147 (1992).
6. D. D. Do, *Chem. Eng. Sci.*, *44*(8), 1707 (1989).
7. M. Giona, M. Giustiniani, and A. Viola, *Chem. Eng. J. Biochem. Eng. J.*, *58*(1), 21 (1995).
8. D. Hyun Kim, *AIChE J.*, *36*(2), 302 (1990).
9. A. K. Jain and A. K. Gupta, *Sep. Sci. Technol.*, *29*(11), 1461 (1994).

10. A. K. Jain, Ph.D. Thesis, I.I.T., Delhi, 1995.
11. S. Joshi and J. R. Fair, *Ind. Eng. Chem. Res.*, *30*(1), 177 (1991).
12. C. S. Leech Jr., *Prod. Finish. (Cincinnati)*, *59*(9), 136 (1995).
13. O. Levenspiel, *Chemical Reaction Engineering*, Wiley, New York, NY, 1964.
14. V. A. Naumov, G. V. Kurgi, and L. V. Maksimova, *Chem. Pet. Eng.*, *26*(3), 135 (1990).
15. L. Riekert, *Chem. Eng. Prog.*, *26*(1), 59 (1989).
16. D. M. Ruthven and J. C. Rojo, *Can. J. Chem. Eng.*, *68*(5), 795 (1990).
17. D. M. Smith, *Ind. Eng. Chem. Fundam.*, *23*, 265 (1984).
18. B. Sowerby and B. D. Crittenden, *Chem. Eng. Res. Des.*, *69*(1), 3 (1991).
19. L. M. Sun, F. Meunier, Ph. Grenier, and D. M. Ruthven, *Chem. Eng. Sci.*, *49*(3), 373 (1994).
20. J. Tantet, M. Eic, and R. Desai, *Gas Sep. Purif.*, *9*(3), 213 (1995).
21. W. K. Teo and D. M. Ruthven, *Ind. Eng. Chem., Prod. Res. Dev.*, *25*, 17 (1986).
22. R. E. Treybal, *Mass Transfer Operations*, McGraw-Hill, New York, NY, 1980.

Received by editor February 2, 1997
Revision received July 1997